Enzyme Engineering

4. Enzyme Reaction Kinetics

4.1 Enzyme Reaction Kinetics & Reactor Design

4.2 Cofactor Regeneration

Enzyme Kinetics

It provides valuable information for enzyme mechanism

It gives an insight into the role of an enzyme under physiological conditions

It can help show how the enzyme activity is controlled and regulated

One Substrate Reactions

One substrate reactions

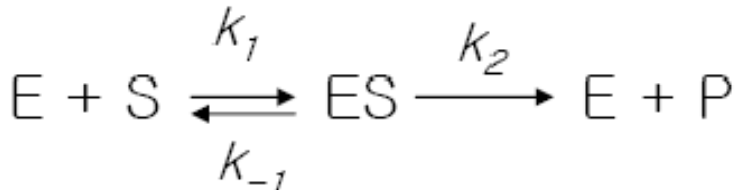

Equilibrium assumption

Second reaction is slower than first reverse reaction($k_{-1} >> k_2$)

$$V_0 = \frac{V_{\max}[S]}{K_s + [S]}$$

Michaelis-Menten eqn

$$K_s = \frac{|E||S|}{[ES]}$$

$$V_{\max} = k_2[E]_0$$

Parameter Estimation

Lineweaver-Burk equation

$$\frac{1}{v} = \frac{K_m}{[S]}\frac{1}{V_{\max}} + \frac{1}{V_{\max}}$$

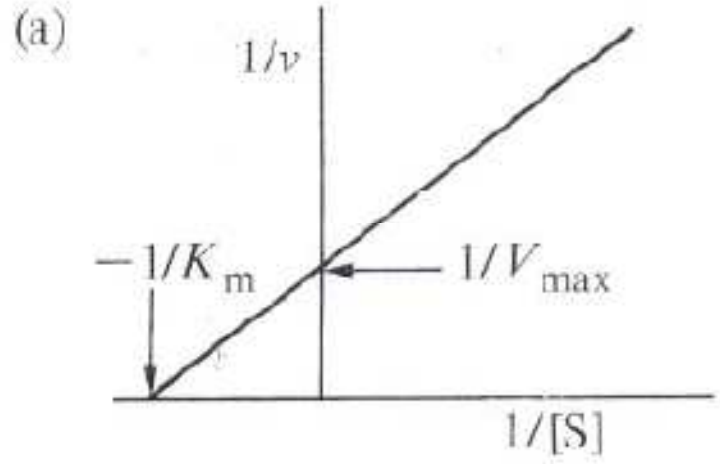

Slope : $\frac{K_m}{[S]}$ Intercept : $\frac{1}{V_{\max}}$

One Substrate Reactions

Significance of the result

1. k_{cat}/K_m is the substrate specificity

$$v_{S_i} = \left(\frac{k_{cat}}{K_m} \right)_{S_i} [E][S_i]$$

2. k_{cat}/K_m can be used for the applicability of equilibrium or steady state assumption

3. K_m is [S] where the rate is (1/2) V_{max}

   - K_m may be the affinity of an enzyme to the substrate(not always)

Batch Kinetics

The time course of variation of [S] in a batch enzymatic reaction can be determined by integrating equation

$$v = \frac{-d[S]}{dt} = \frac{V_m[S]}{K_m + [S]}$$

integration

$$V_m t = [S_0] - [S] + K_m \ln \frac{[S_0]}{[S]}$$

Or,

$$V_m - \frac{[S_0] - [S]}{t} = \frac{K_m}{t} \ln \frac{[S_0]}{[S]}$$

A plot of $1/t([\ln[S_0]/[S])$ versus $\{[S_0]-[S]\}/t$ results in a line of slope $-1/K_m$ with a y-intercept of V_m/K_m

Inhibition

Inhibition of enzyme activity

Competitive inhibition

- Binding into active site

Non-competitive inhibition

- Binding outside active site

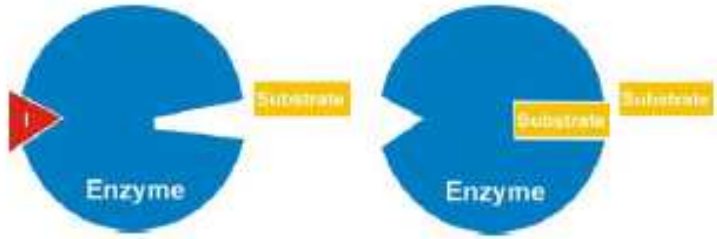

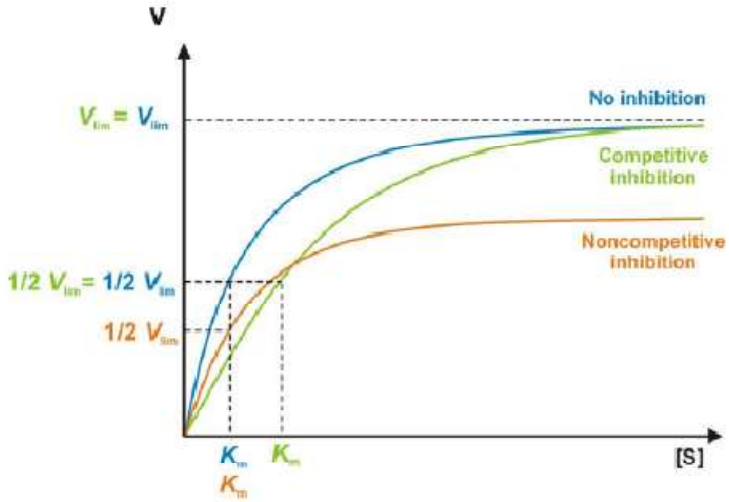

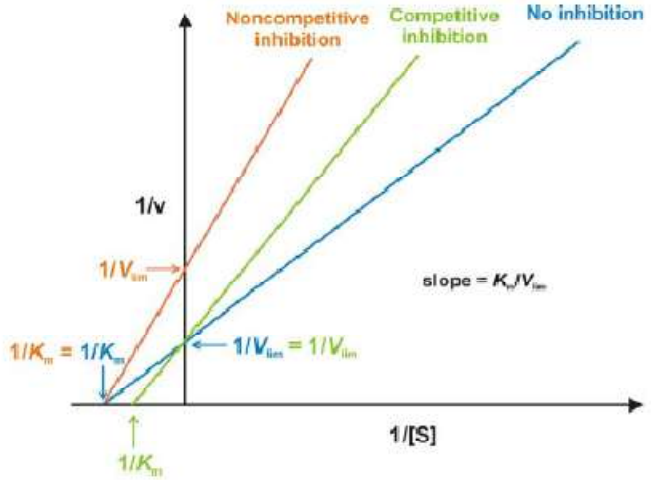

Inhibition

Competitive inhibition

$$E + S \underset{k_{-1}}{\overset{k_1}{\longleftrightarrow}} ES \xrightarrow{k_2} E + P$$

$$+$$

$$I$$

$$\updownarrow K_I$$

$$EI$$

$$v = \frac{V_m[S]}{K_m^{'}[1 + \frac{[I]}{K_I}] + [S]}$$

Non-competitive inhibition

$$E + S \underset{K_m^{'}}{\longleftrightarrow} ES \xrightarrow[k_2]{} E + P$$

$$+ \qquad\qquad +$$

$$I \qquad\qquad I$$

$$K_I \updownarrow \qquad\qquad K_I \updownarrow$$

$$EI + S \underset{K_m^{'}}{\longleftrightarrow} ESI$$

$$v = \frac{V_m}{(1 + \frac{[I]}{K_1})(1 + \frac{K_m^{'}}{[S]})}$$

Substrate Inhibition

Substrate inhibition

High substrate concentrations may cause inhibition in some enzymatic reactions

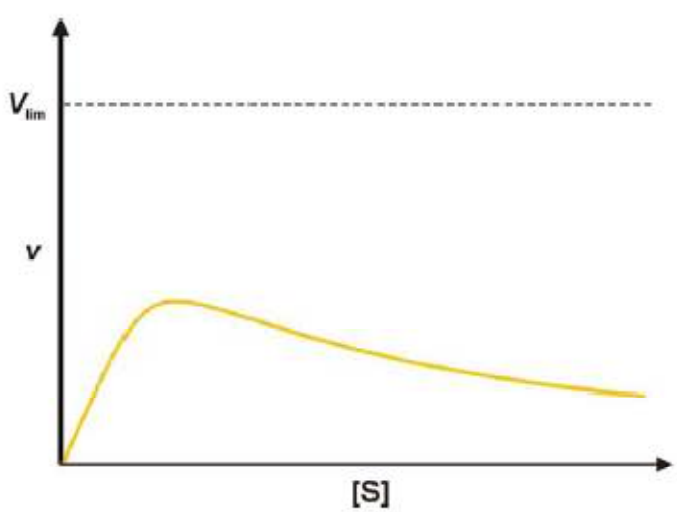

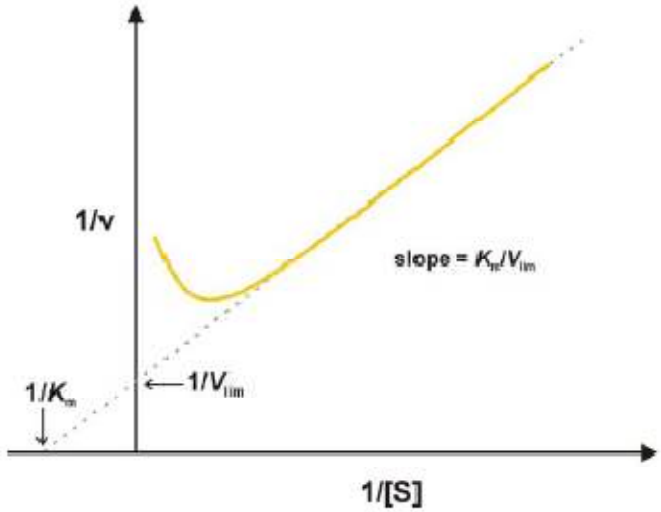

Substrate Inhibition

Substrate inhibition

$$E + S \underset{}{\overset{K_m'}{\longleftrightarrow}} ES \xrightarrow{k_2} E + P$$

$$+$$

$$S$$

$$\updownarrow K_{S_1}$$

$$ES_2$$

$$v = \frac{V_m[S]}{K_m' + [S] + \frac{[S]^2}{K_{S1}}}$$

At low [S], $[S]^2/K_{S_1}$<<1, no inhibition

$$v = \frac{V_m}{[1 + \frac{K_m'}{[S]}]}$$

Effect of Temperature

Effect of temperature

Effect on enzyme structure

-Denaturation(unfolding)

-Structural change in active site

Effect on enzyme catalysis

- Catalytic rate generally increase with temperature

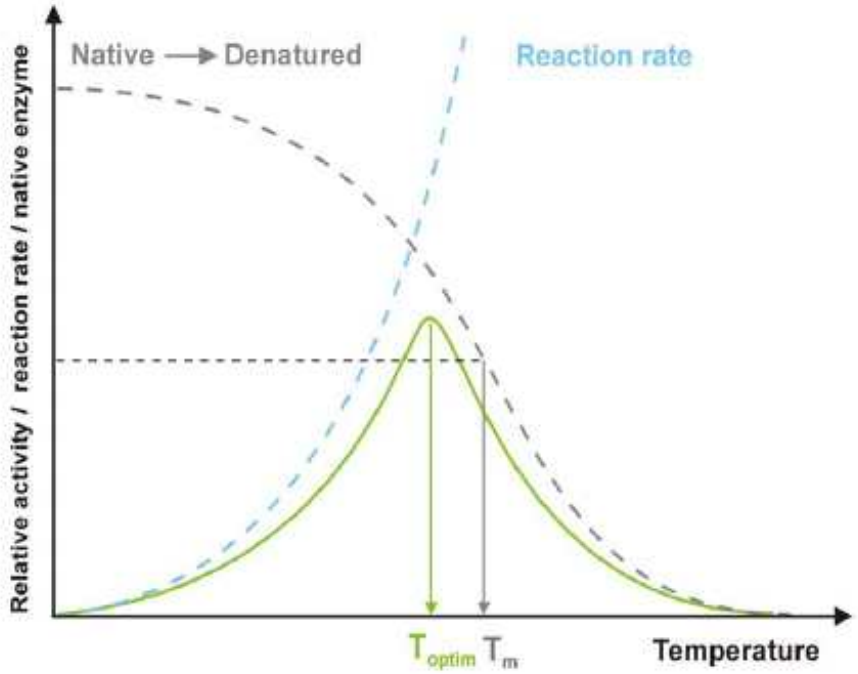

Effect of pH

Effect of pH

pH optimum and specific range of activity

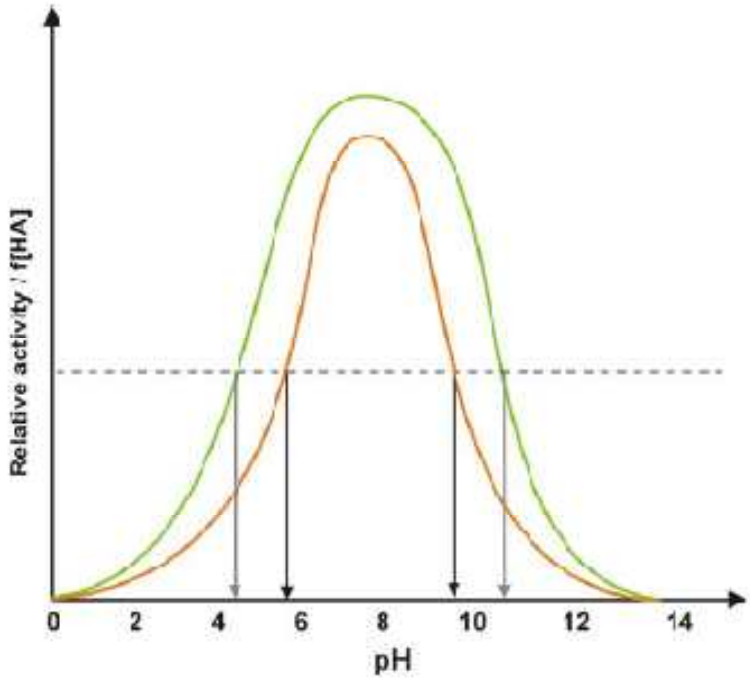

Parameter Estimation

Bioreactor Design Eqn

4.2 Cofactor Regeneration

Biocatalysis cycle

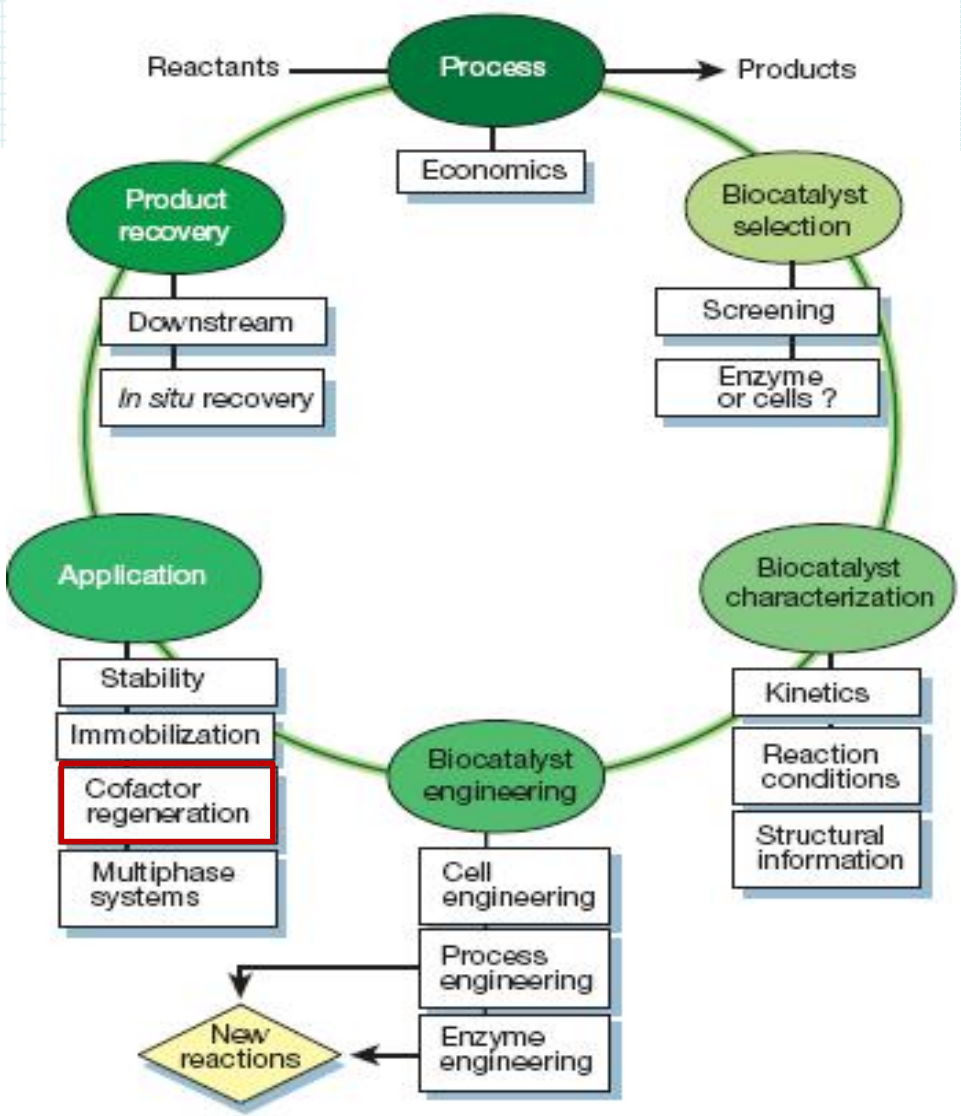

Nature 2001, 409, 258-268

Common cofactors required for biotransformation and their representative *in situ* regeneration methods

Cofactor	Enzyme	Reaction type	Representative regeneration method
NAD^+/NADH	Oxidoreductase	Removal or addition hydrogen	Glutamate dehydrogenase with α-ketoglutarate/ Formate dehydrogenase with formate
$NADP^+$/NADPH	Oxidoreductase	Removal or addition hydrogen	Glutamate dehydrogenase with α-ketoglutarate/ Glucose dehydrogenase with glucose
ATP	Kinase, synthase	Phosphorylation	Acetate kinase with acetyl phosphate
Sugar nucleotides	Kinase, synthase	Glycosyl transfer	Bacterial coupling
Acetyl CoA	Dehydrogenase, Transferase, Synthase	Acyl transfer (C2-alkylation)	Phosphotransacetylase with acyl phosphate
PAPS	Transferase	Sulfuryl transfer	Aryl sulfotransferase IV with p-nitrophenyl sulfate
SAM	Dehydrogenase, Transferase, Synthase	Methyl transfer (C1-alkylation)	No demonstrated method
Flavins[a]	Oxygenase, hydroxylase	Oxygenation	Self-regeneration
Pyridoxal phosphate	Transaminase	Transamination	Self-regeneration
Biotin	Carboxylase, Decarboxylase	Carboxylation	Self-regeneration
Metal porphyrin complexes[a]	Monooxygenase, Peroxidase, Mutase	Peroxydation, oxygenation	Self-regeneration

[a]Many flavin- and metal porphyrin complexes dependent mono- or dioxygenases require additional NAD(P)H as an indirect reducing agent.

Biotransformations in Organic Chemistry, 2004
Current Opinion in Biotechnology, 2003,14(6), 583-589

Oxidoreductase

- Oxidoreductases are valuable enzymes which have potential in synthesizing many kinds of chemicals used in pharmaceutical applications, food additives, etc. (amino acids, chiral alcohols, ketones, steroids, etc.)

- Especially, enzymatic oxidation by oxidoreductase is attractive due to myriad of applications for the organic synthesis as well as analytical purpose including clinical diagnosis and fuel generation.

Structure of nicotinamide cofactors

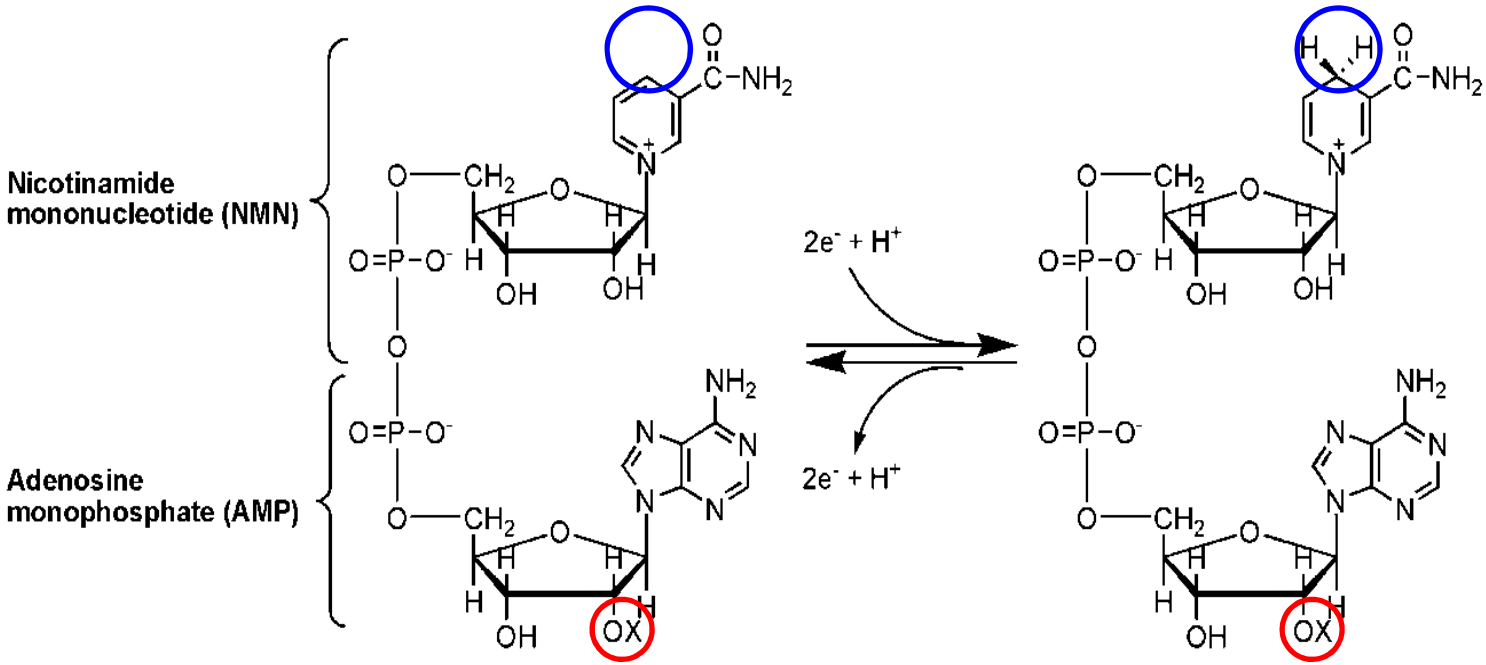

Necessity of cofactor regeneration

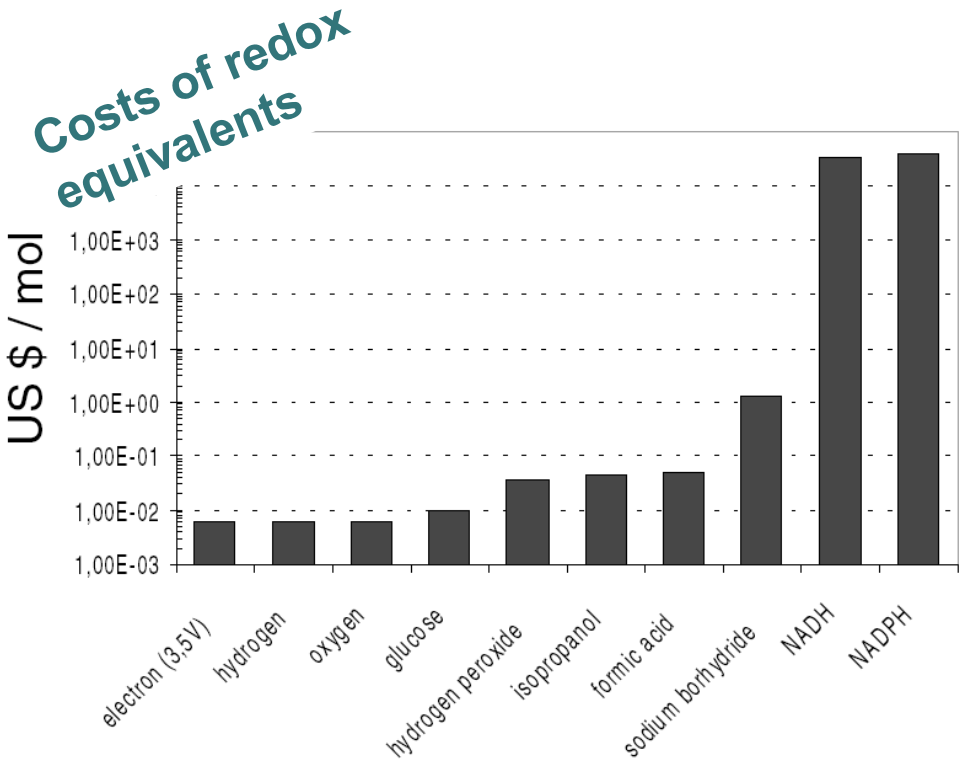

The Chemical Record 2004, 4, 254-265

Table. Cost of nicotinamide cofactor.

	Cost (US dollar) / g	Cost (US dollar) / mol
NAD^+	56	37,150
NADH	97	68,599
$NADP^+$	344	263,298
NADPH	1,080	900,018

http://www.sigmaaldrich.com (2009)

Strategies for cofactor regeneration

Method	Advantage	Disadvantage
Enzymatic method	• High selectivity • Compatibility	• High enzyme cost • Enzyme instability • Complexity of product isolation
Electrochemical method	• Low cost of electricity • No stoichiometric regenerating reagent • Easy product isolation • Clean process	• Complex apparatus and procedure • Requirement in many systems for mediating redox agent
Chemical method	• Commercially available reagents • No requirement for added enzyme	• Incompatibility • Complexity of product isolation • Low product yield • Low TTN
Photochemical method	• No stoichiometric regenerating reagent in some systems • No requirement for added enzymes	• Complex apparatus • Incompatibility • Limited stability • Requirement for photosensitizer and redox dyes

Enzymatic regeneration of NAD+

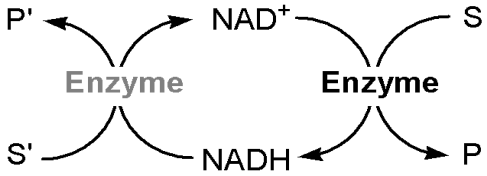

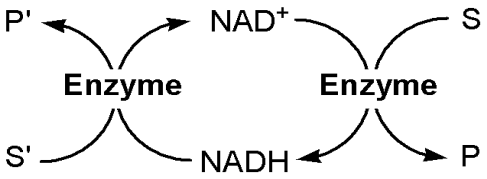

Enzyme: production enzyme
Enzyme: cofactor regeneration enzyme

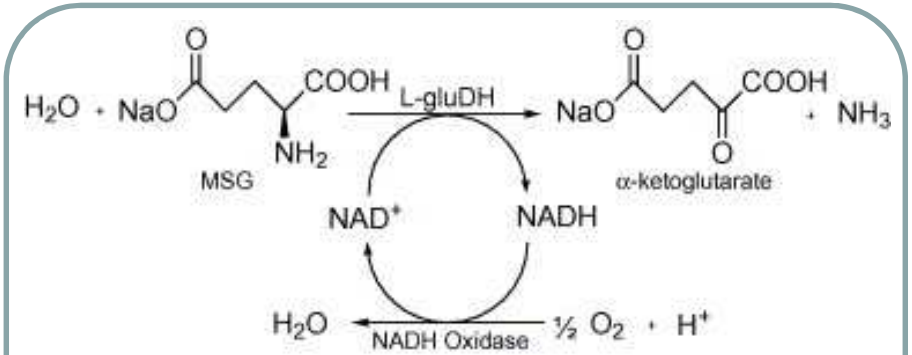

Tetrahedron: Asymmetry 2004,15(18), 2933-2937

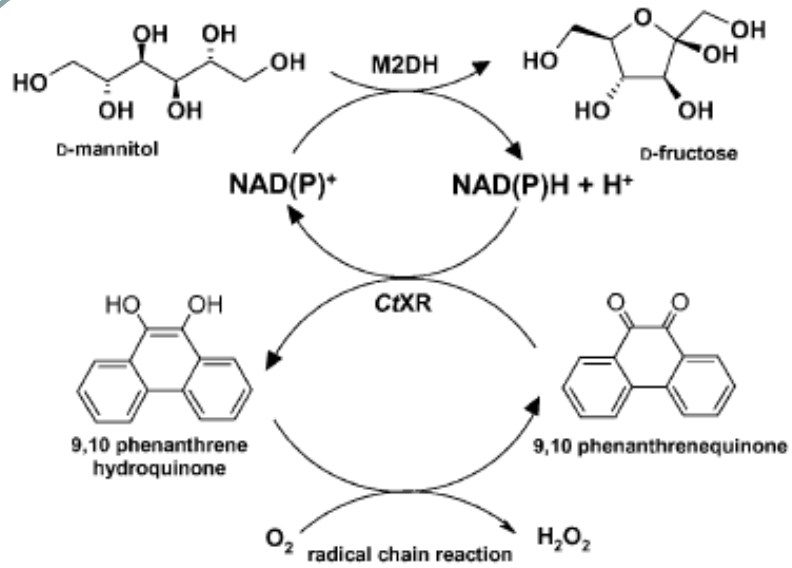

Adv. Synth. Catal. 2008, 350, 2305-2312

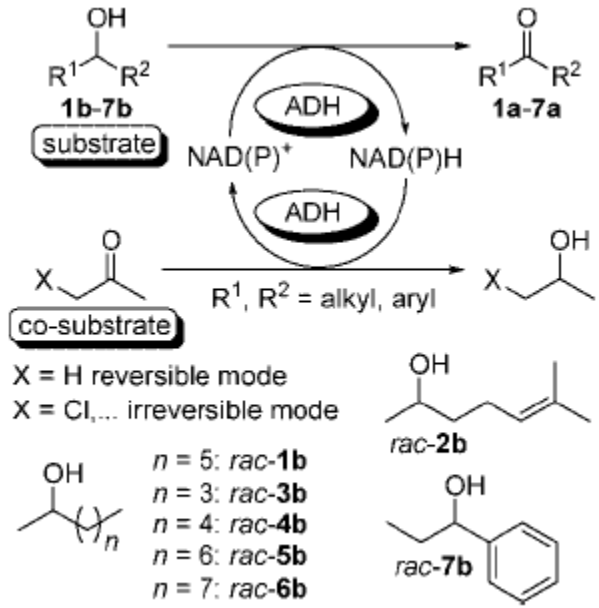

Strategies for cofactor regeneration

Method	Advantage	Disadvantage
Enzymatic method	• High selectivity • Compatibility	• High enzyme cost • Enzyme instability • Complexity of product isolation
Electrochemical method	• Low cost of electricity • No stoichiometric regenerating reagent • Easy product isolation • Clean process	• Complex apparatus and procedure • Requirement in many systems for mediating redox agent
Chemical method	• Commercially available reagents • No requirement for added enzyme	• Incompatibility • Complexity of product isolation • Low product yield • Low TTN
Photochemical method	• No stoichiometric regenerating reagent in some systems • No requirement for added enzymes	• Complex apparatus • Incompatibility • Limited stability • Requirement for photosensitizer and redox dyes

Electrochemical regeneration of NAD^+

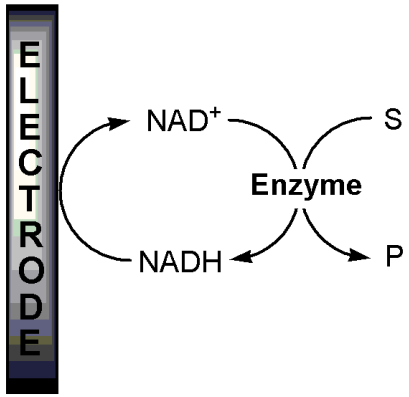

Direct oxidation of NADH

- Cofactors to be regenerate itself on the electrode surface
- Requires high overpotential
- Lead to undesired side-reactions

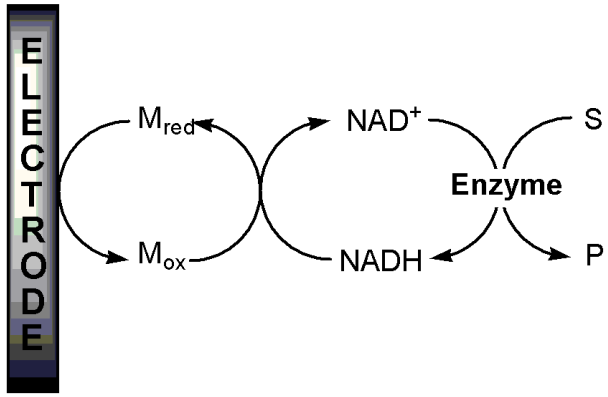

Mediated oxidation of NADH

- Low overpotential
- Redox mediators catalyzing the electron transfer
- Used as soluble mediators as well as immobilized on the electrode surface

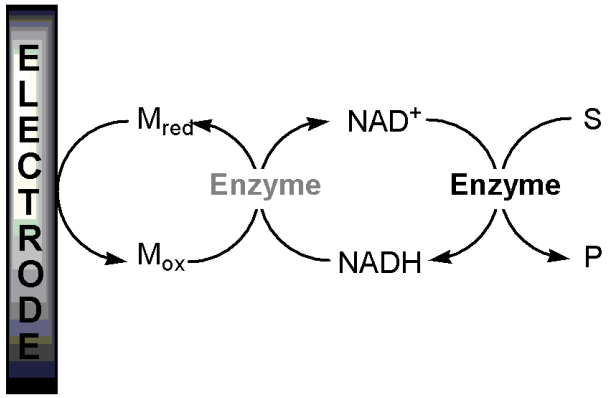

Indirect electroenzymatic oxidation of NADH

- Accelerate electron transfer kinetics from NAD(P)H to the oxidized mediator by enzymatic catalysis

Electroenzymatic synthesis

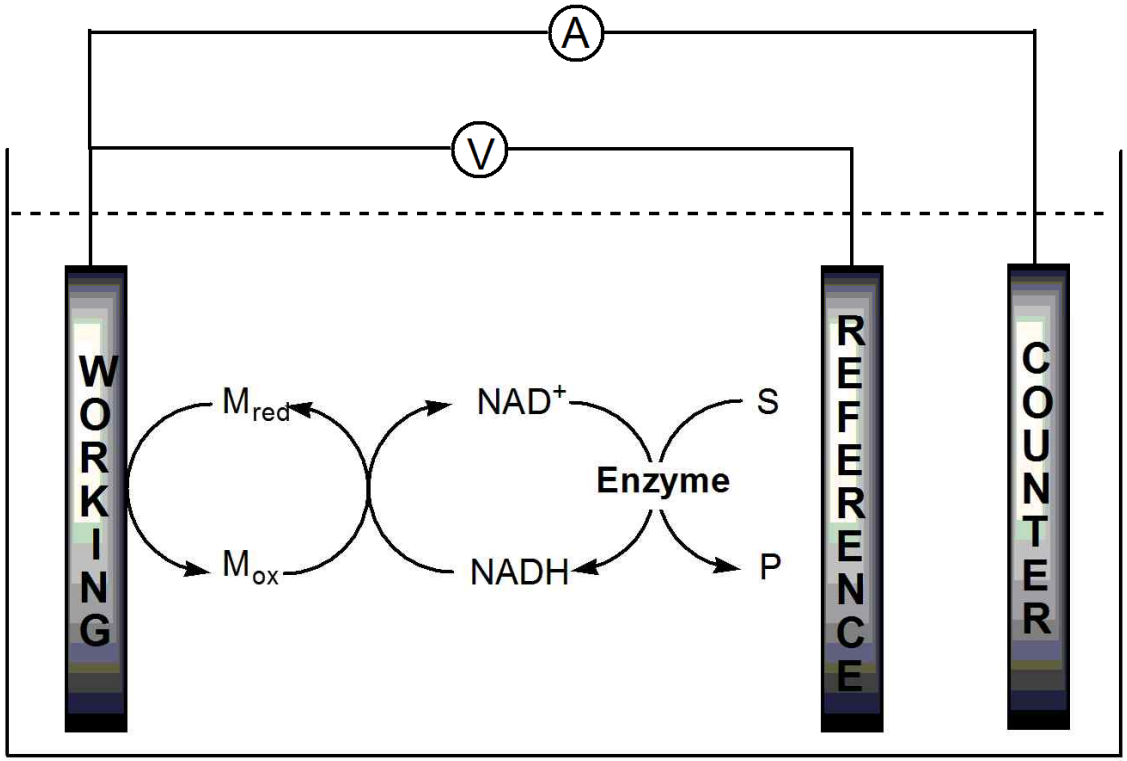

Enzyme (cofactor)	Mediator/enzyme	Substrate	Product	Electrode	E_{appl}	Remarks	Reference
Mediator-free system							
NAD^+-glucose dehydrogenase	-	glucose	gluconate	Cylinder type of RVC	+0.8 V vs. SCE	TTN_{cof}>10 000 TOF_{cof}=225±7 h^{-1} Yield=99.99%	Bonnefoy et al., 1988
NAD^+-lactate dehydrogenase	-	L-lactate	D-lactate	Carbon felt (anode) Mercury (cathode)	+0.5 V vs. SCE (anode) -1.75 V vs. SCE (cathode)	97 % conversion	Biade et al., 1992
$NAD(P)^+$-glucose dehydrogenase	-	glucose	gluconate	Graphite felt	+0.7 V vs. Ag/AgCl	Maximum substrate consumption rate (r_s) r_s=32 µmol min^{-1} (w/o PEI) r_s=59 µmol min^{-1} (w/ PEI)	Obón et al., 1997
NAD^+-alanine dehydrogenase	-	L-alanine	D-alannine	Carbon felt (anode) Hg pool (cathode)	+0.5 V vs. SCE (anode) -1.350 V vs. SCE (cathode)	100% conversion (140 h)	Anne et al., 1999
$NADP^+$-alcohol dehydrogenase	-	2-propanol	Acetone	Anodic tin oxide	-0.5 V vs. Ag/AgCl	91% conversion (51 h)	Kim et al., 2009
NAD^+-alcohol dehydrogenase	-	(*rac*)-2-pentanol	(*R*)-2-pentanol	Anodic tin oxide	-0.5 V vs. Ag/AgCl	50% conversion (9 h) ee>99% Productivity = 0.03 g l^{-1} h^{-1} Max. productivity = 0.16 g l^{-1} h^{-1}	Kim and Yoo, 209
Mediated system							
NAD^+-alcohol dehydrogenase	$Fe(tmphen)_3^{2+}$	2-hexen-1-ol	2-hexenal	Graphite felt	+0.63 V vs. Ag/AgCl	C_{prod}=1.77 mM (60 min) TTN_{cof}=18[1] TTN_{med}=36 Current efficiency=90%	Komoschinsk and Steckhan, 1988
$NADP^+$-alcohol dehydrogenase	$Fe(tmphen)_3^{2+}$	2-butanol	2-butanone	Graphite felt	+0.63 V vs. Ag/AgCl	C_{prod}=4.1 mM (150 min) TTN_{cof}=41 TTN_{med}=82 Current efficiency=95%	Komoschinsk and Steckhan, 1988
NAD^+-alcohol dehydrogenase	Tris(1,10-phenanthroline-5,6-dione) ruthenium (II) perchlorate	cyclohexanol	cyclohexanone	Carbon foil	+0.1 V vs. Ag/AgCl	TOF=35 h^{-1} (aerobic, 60 min) TOF=28 h^{-1} (anaerobic)	Hilt and Steckhan, 1993
NAD^+-alcohol dehydrogenase	$[Co(tren)(phendi)](BF_4)_2$	cyclohexanol	cyclohexanone	Carbon foil	+0.1 V vs. Ag/AgCl	TOF=81 h^{-1} (aerobic, 60 min)	Hilt and Steckhan, 1993
NAD^+-alcohol dehydrogenase	$ABTS^{2-}$	*meso*-3,4-dihydroxymethylcyclo hex-1-ene	(3a*R*,7a*S*)-3a4,7,a-tetrahydro 3H-isobenzofurane-1-one	Carbon felt	+0.585 V vs. Ag/AgCl	ee>99.5% 93.5 % conversion (46.5 h) Productivity=3.24 g l^{-1} d^{-1} TTN_{med}=30.4	Schröder et al., 2003
NAD^+-glycerol dehydrogenase	$ABTS^{2-}$	1-phenyl-1,2-ethanediol	(*S*)- 1-phenyl-1,2-ethanediol	Carbon felt	+0.585 V vs. Ag/AgCl	-	Degenring et al., 2004
Electroenzymatic system							
$NADP^+$-isocitrate dehydrogenase	CAV/AMAPOR	(*rac*)-isocitrate	(2*S*, 3*S*)-isocitrate	graphite	-0.2 V vs. SCE	Productivity number=13 000 mmol kg^{-1} h^{-1} (3.8 h) ee>99 %	Schulz et al., 1995
$NADP^+$-isocitrate dehydrogenase	AQ-S/AMAPOR	(*rac*)-isocitrate	(2*S*, 3*S*)-isocitrate	graphite	-0.2 V vs. SCE	Productivity number=14 000 mmol kg^{-1} h^{-1} (3.6 h) ee>99 %	Schulz et al., 1995
$NADP^+$-6-phosphogluconate dehydrogenase	CAV /AMAPOR	6-phosphogluconate	ribose 5-phosphate	graphite	-0.2 V vs. SCE	80% conversion (2.3 h) (crude extract AMAPOR) 98% conversion (2.5 h) (partially enriched AMAPOR)	Schulz et al., 1995

Current problems of electrochemical regeneration system

- Enzymes can be easily deactivated on the electrode surface.
- The overall reaction is often limited by the cofactor regenerate rate which is usually much slower than the enzymatic reaction rate.
- Used materials for mediator are often toxic to enzyme causing enzyme deactivation.
- The stability of the mediator is affecting the performance and stability of the process.

Metal oxide electrode

Improvement of electrochemical reaction rate

↓

Enlargement of electrode surface area

↓

Porous electrode

↓

Anodic metal oxide??

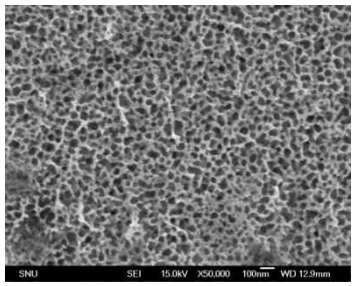

Figure. FE-SEM image of tin oxide

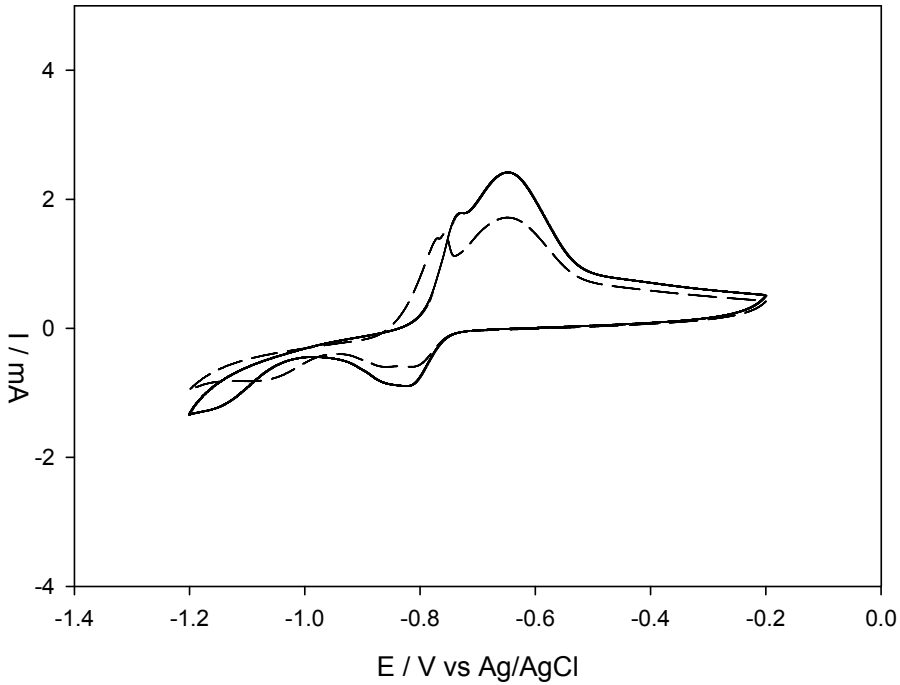

Figure. Cyclic voltammograms of tin oxide in the absence (---) and presence (—) of 0.5 mM NADH. Conditions: 100 mM potassium phosphate buffer (pH 7.5), scan rate=20 mV sec^{-1}, electrode size=5 cm^2.

Enzyme and Microbial Technology, 2009, 44(3), 129-134

Cyclic voltammogram of metal oxide

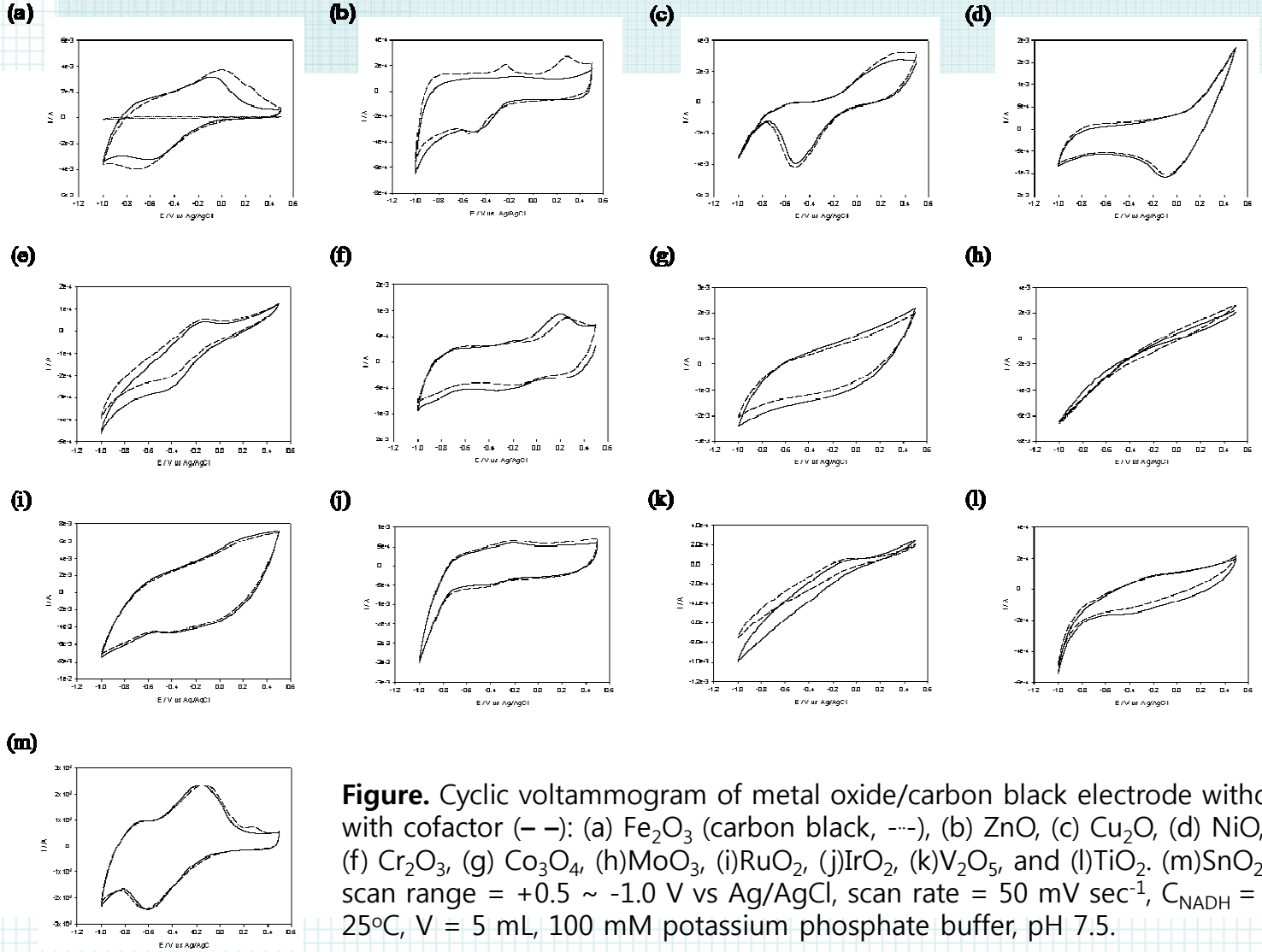

Figure. Cyclic voltammogram of metal oxide/carbon black electrode without (—) and with cofactor (– –): (a) Fe_2O_3 (carbon black, ···-), (b) ZnO, (c) Cu_2O, (d) NiO, (e) Mn_3O_4, (f) Cr_2O_3, (g) Co_3O_4, (h)MoO_3, (i)RuO_2, (j)IrO_2, (k)V_2O_5, and (l)TiO_2. (m)SnO_2Conditions: scan range = +0.5 ~ -1.0 V vs Ag/AgCl, scan rate = 50 mV sec^{-1}, C_{NADH} = 1 mM, T = 25°C, V = 5 mL, 100 mM potassium phosphate buffer, pH 7.5.

Comparison of NAD^+ and $NADP^+$ regeneration according to metal oxide electrode

Metal oxide	Applied potential [V vs. Ag/AgCl]	NAD^+ regeneration			$NADP^+$ regeneration		
		Reaction rate[a] [μM min^{-1}]	Current efficiency [%]	Relative activity[b] [%]	Reaction rate[a] [μM min^{-1}]	Current efficiency [%]	Relative activity[c] [%]
IrO_2	-0.15	5.7	54	99.29±1.14	10.6	54	109.93±0.69
Mn_3O_4	-0.05	3.6	66	96.93±3.94	3.7	64	100.54±1.10
Fe_2O_3	+0.05	3.1	>99	98.80±0.14	1.3	>99	97.45±7.03
ZnO	+0.30	5.6	81	95.39±2.16	9.2	74	96.88±2.98
Cr_2O_3	+0.30	7.1	84	99.28±4.18	7.8	77	100.46±0.66
SnO_2	+0.30	3.6	71	97.24±1.58	4.6	85	96.72±4.46
Cu_2O	+0.43	6.3	42	102.23±3.10	7.5	27	97.40±1.09

[a] initial reaction rate (R^2>0.995)
[b] relative activity of regenerated cofactor to NAD^+-dependent glutamate dehydrogenase
[c] relative activity of regenerated cofactor to $NADP^+$-dependent alcohol dehydrogenase

Mechanism of NADH oxidation

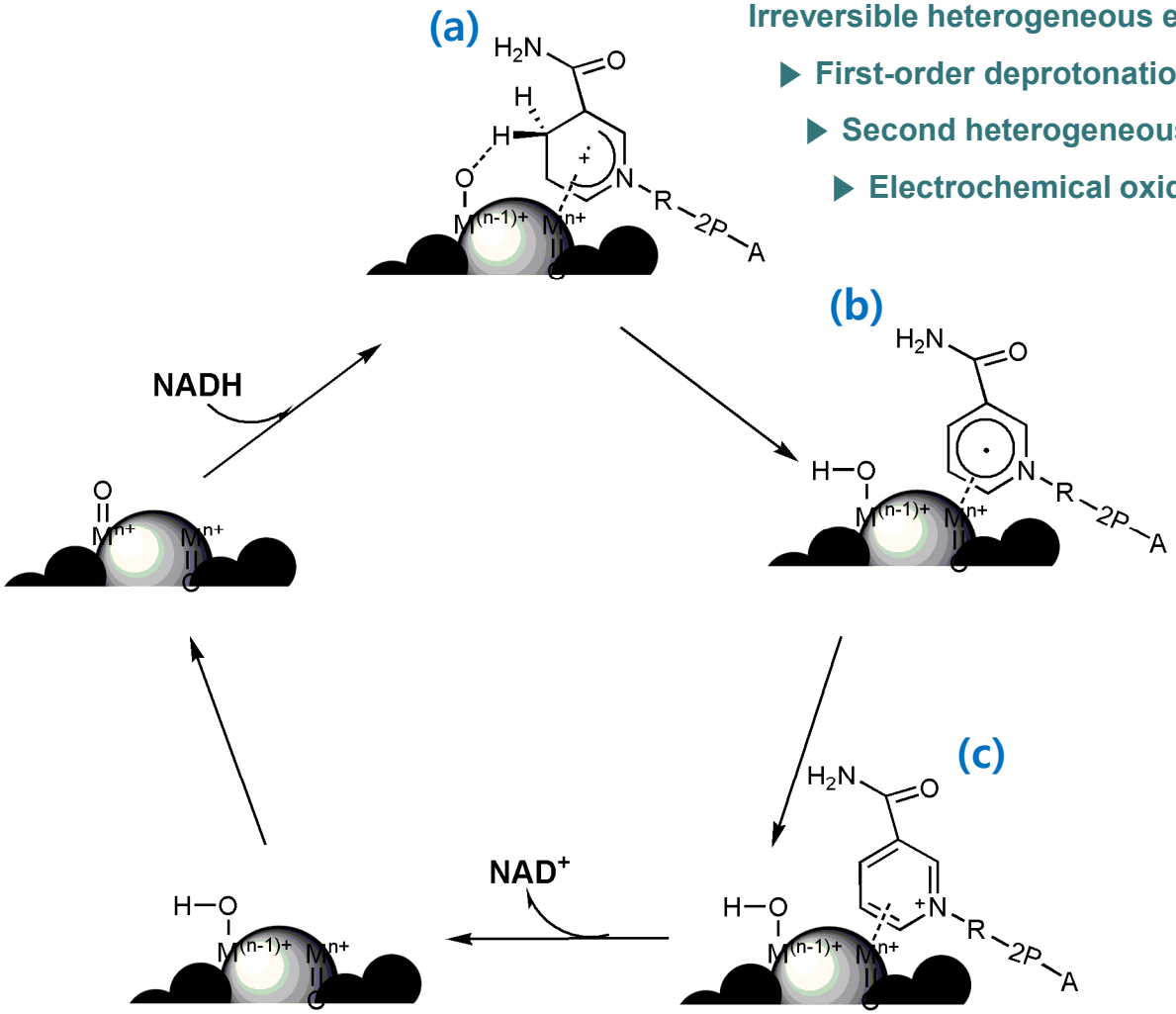

Irreversible heterogeneous electron transfer (a)

- First-order deprotonation reaction (b) (metal oxide reduction)
  - Second heterogeneous electron transfer (c)
    - Electrochemical oxidation of metal oxide

Electroenzymatic oxidation of (*rac*)-2-pentanol

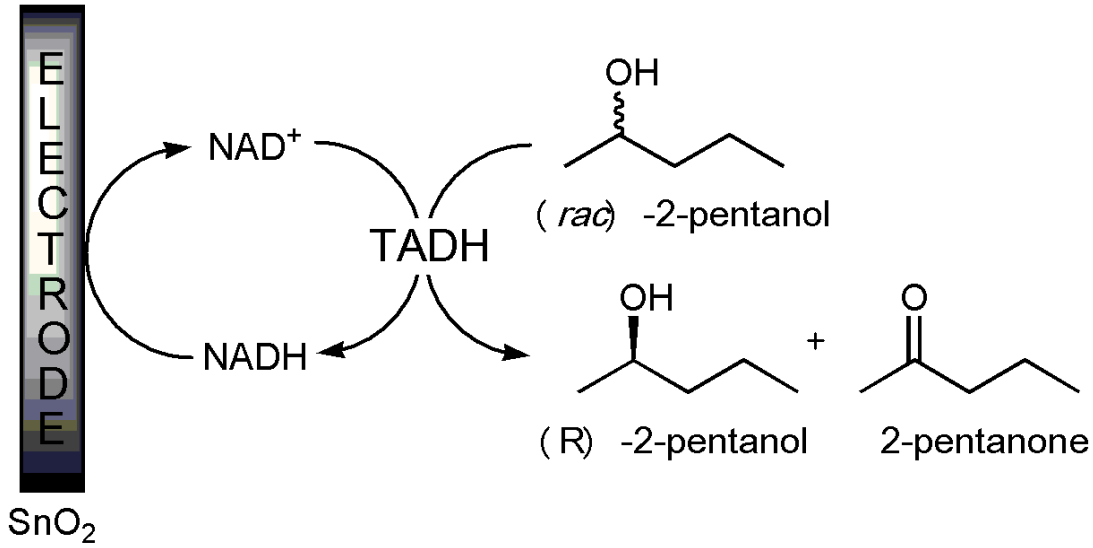

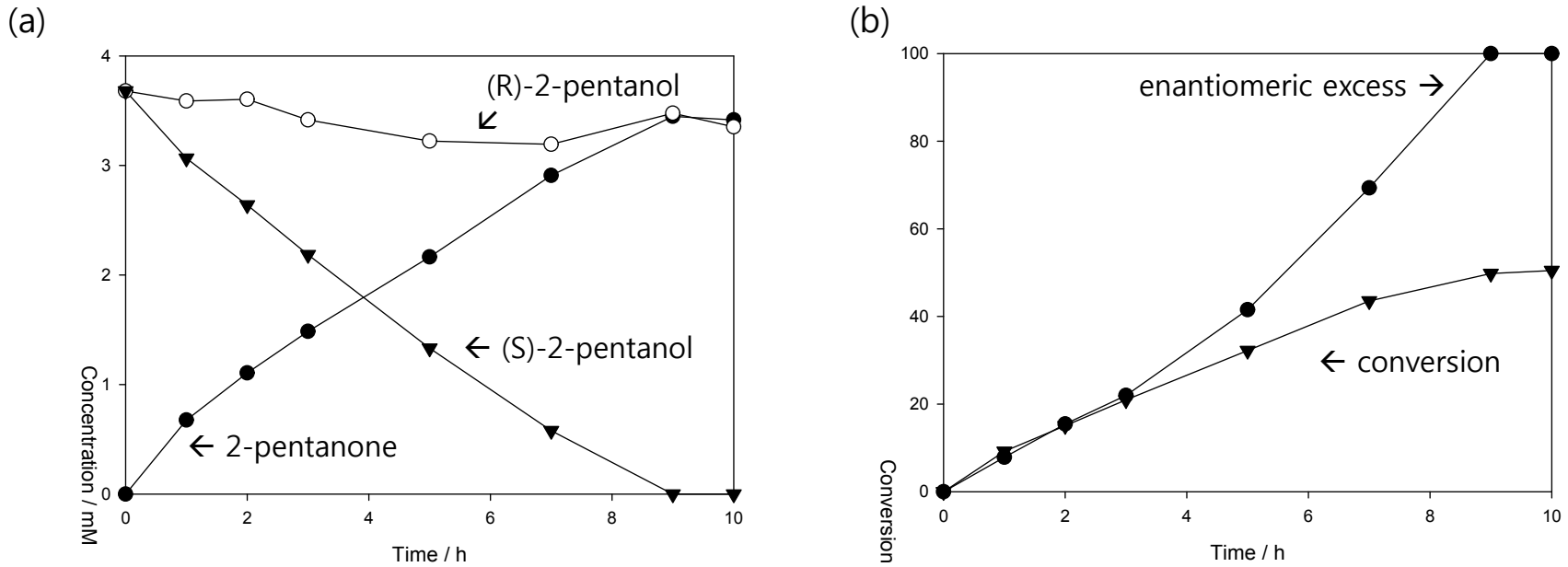

Figure. (a) Kinetic resolution of low concentration of (*rac*)-2-pentanol by electroenzymatic oxidation: ●, 2-pentanone; ○, (*R*)-2-pentanol; ▼, (*S*)-2-pentanol. (b) Conversion and enantiomeric excess of electroenzymatic kinetic resolution: ●, enantiomeric excess; ▼, conversion. *Reaction conditions*: 100 mM potassium phosphate buffer, pH 8.2, T=50°C, V=15 mL, applied potential: -0.5 V vs Ag/AgCl, electrode surface area=4 cm^2, C_{TADH}=2 U mL^{-1}, C_{NAD^+}=0.5 mM, $C_{(rac)\text{-}2\text{-}pentanol}$=7.3 mM.

Electroenzymatic deamination of L-glutamate

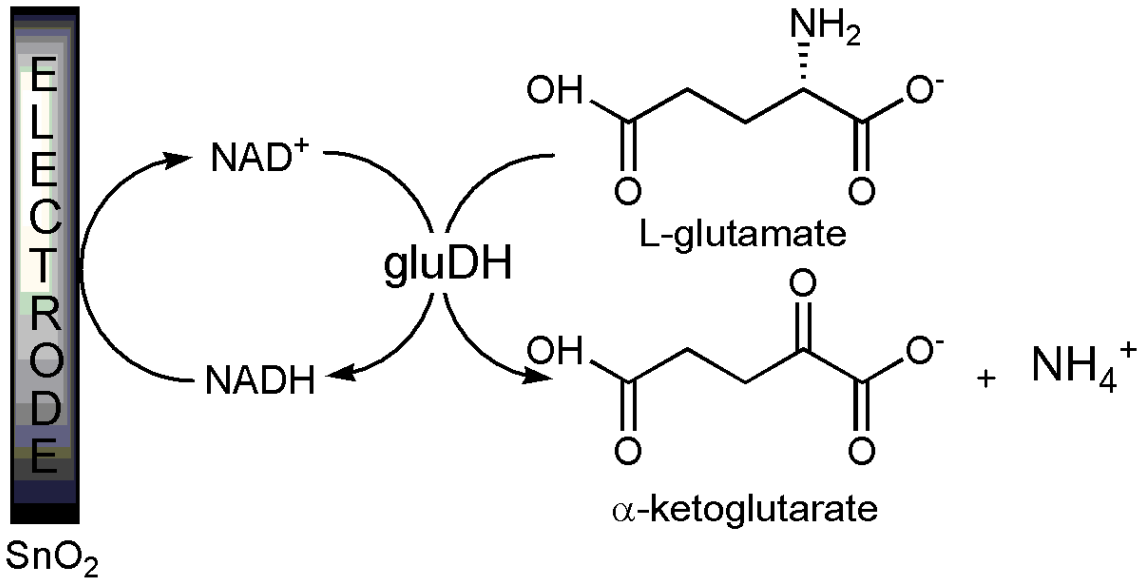

Continuous type of electrochemical bioreactor

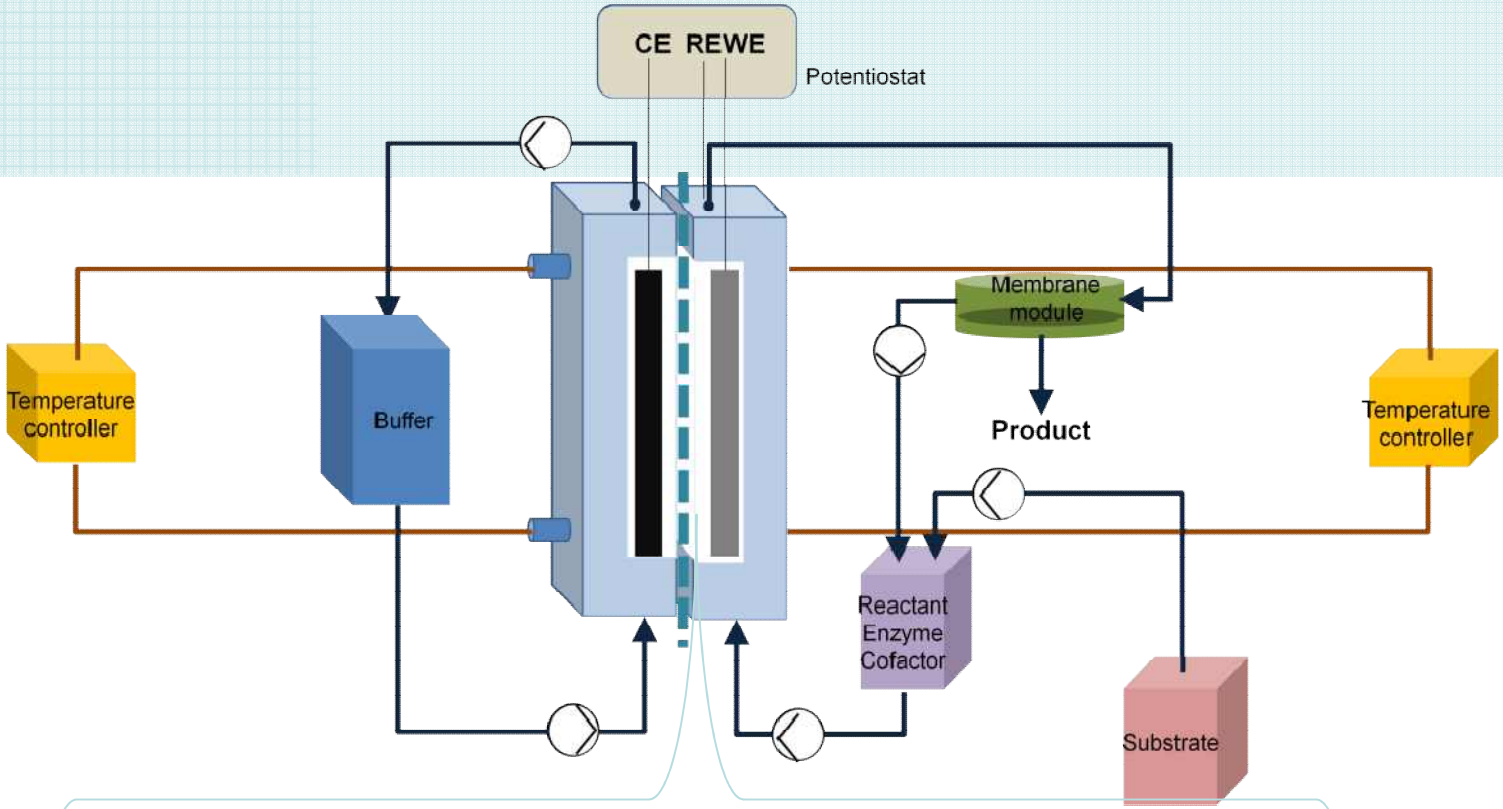

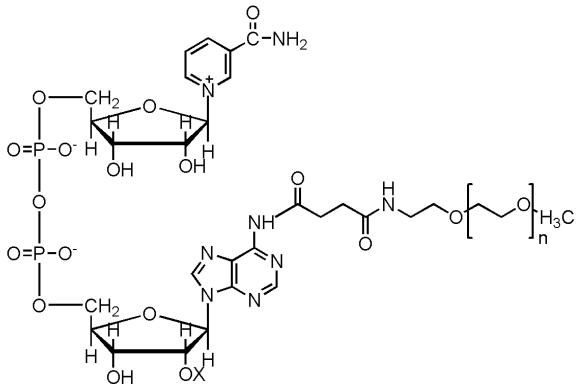

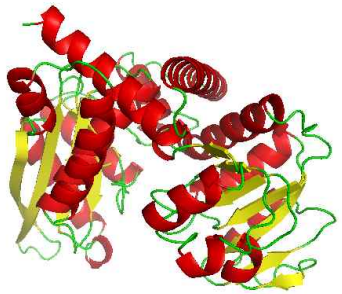

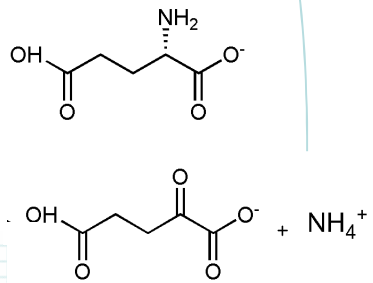

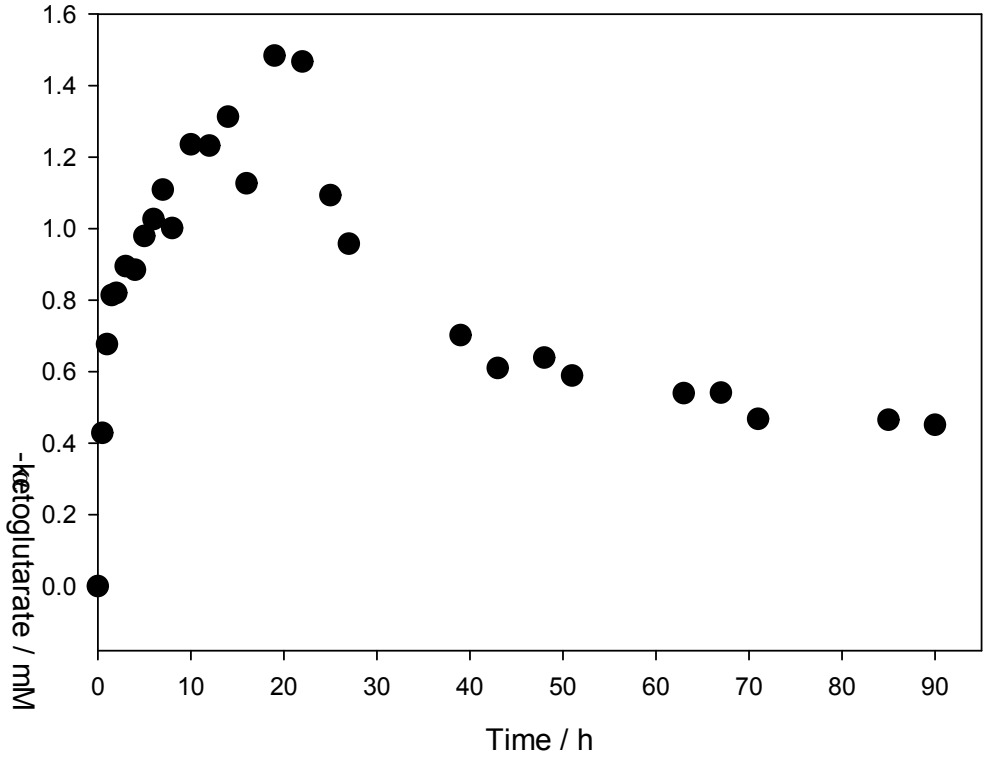

Figure. Continuous synthesis of α-ketoglutarate using electrochemical bioreactor. Conditions: 100mM CHES buffer (pH 9.0), C_{gluDH} = 3.87 U ml^{-1}, $C_{PEG\text{-}NAD+}$ = 0.33 mM, C_{MSG} = 5 mM, flow rate = 1 ml min^{-1}, T = 60°C.

Biosensor

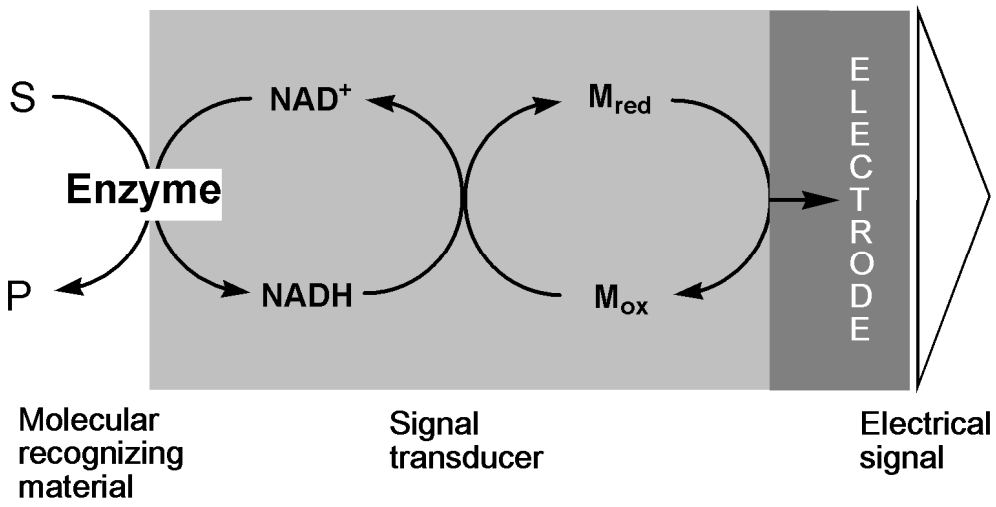

- Measuring NADH is very important because NAD(P)$^+$ is used as a cofactor for about 250 NAD$^+$-dependent and 150 NADP$^+$-dependent dehydrogenases.
- It can be applied to analytical detection, fermentation, clinical practices, food industry, and dairy industry.

Analyte	Enzyme	Electrode	Electrode modified material or mediator	E_{appl}	LOD (S/N=3) [μM]	Linear range [μM]	Sensitivity	Reference
Mediated system								
Ethanol	Alcohol dehydrogenase	Pt	Phenazine methosulphate (PMS^+)	+0.314 V vs. Ag/AgCl	0.3	-500	810nA mol^{-1}	Malinauskas and Kulys, 1977
D,L-lactate	Lactate dehydrogenase				-	-1500	14nA mol^{-1}	
L-glutamate	Glutamate dehydrogenase				-	-100000	50 nA mol^{-1}	
Ethanol	Alcohol dehydrogenase	Carbon paste	Meldola blue adsorbed on silica gel modified with niobium oxide (SNMB)	+0.00 V vs. SCE	8	100-10000	2.3 μA cm-2 mM^{-1}	Santos et al., 2003
Lactate	Lactate dehydrogenase				6.5	100-14000	2.4 μA cm^{-2} mM^{-1}	Pereia et al., 2006
Ethanol	Alcohol dehydrogenase	Carbon nanotube paste	Meldola blue adsorbed on multiwall carbon nanotube (MWCT-MB)	+0.00 V vs. SCE	5	50-10000	4.75 μA cm^{-2} mM^{-1}	Santos et al., 2006
L-lactate	Lactate dehydrogenase	GC	Meldola blue (MB)	+0.25 V vs. Ag/AgCl	1.5	-	1.47 μM mM^{-1}	Lin et al., 2007
Ethanol	Alcohol dehydrogenase	GC	Methylene green (MG)	+0.05 V vs. SCE	12	20-350	-	Dai et al., 2008
Lactate	Lactate dehydrogenase	graphite	Meldola blue coimmobilized on multi-wall carbon nanotube (MB-MWCNT)	+0.00 V vs. SCE	-	100-10000	3.46 μA cm^{-2} mM^{-1}	Pereira et al., 2007
Mediator-free system								
Lactate	Lactate dehydrogenase	GC	Poly(aniline)-poly(acrylate) film Poly(aniline)-poly(vinyl sulfonate) film	+0.05 V vs. SCE	-	-	-	Halliwell et al., 2002
Ethanol	Alcohol dehydrogenase	Composite electrode	Colloidal gold-multiwall carbon nanotube (Au_{coll}-MWCNT-Teflon)	+0.3 V vs. Ag/AgCl	4.7	0.01-1.00	-	Manso et al., 2007
Glucose	Glucose dehydrogenase	ITO	Thionine bridged carbon nanotubes and gold nanoparticles multilayer (MWNTs/thionine/AuNPs)	+0.2 V vs. Ag/AgCl	5.0	10-2560	7.8 μA mM^{-1} (w/o light)	Deng et al., 2008
					0.7	1-3250	18.5 μA mM^{-1} (w/ light)	
Ethanol	Alcohol dehydrogenase	ITO	Gold nanoparticles loaded poly(3,4-ethylenedioxythiophene)-poly(styrene sulfonic acid) film (PEDOT-PSS-Au_{nano})	+0.04 V vs. SCE	-	-	97 mA M^{-1} cm^{-2}	Manesh et al., 2008
Ethanol	Alcohol dehydrogenase	ITO	Au nanoparticle	Potential step -0.2 V-0.1 V vs. SCE	-	-	-	Shlyahovsky et al., 2005
Ethanol	Alcohol dehydrogenase	GC	Poly(vinyl alcohol)-multiwalled carbon nanotube (PVA-MWCNT)	+0.6 V vs. Ag/AgCl	-	~1500	196 nA mM^{-1}	Tsai et al., 2007
Lactate	Lactate dehydrogenase	Au	Gold nanoparticle (AuNP)	-0.065 V vs. Ag/AgCl	0.1	0-800	0.446 nA nM^{-1}	Jena and Raj, 2007
Ethanol	Alcohol dehydrogenase	GC	Soluble carbon nanofiber	+0.06 V vs. SCE	3.0	10-435	-	Wu et al., 2007
Glucose	Glucose dehydrogenase	GC	Carbon nanotube-chitosan film (CNT-CHIT)	+0.3 V vs. Ag/AgCl	3	5-300	80 mA M^{-1} cm^{-2}	Zhang et al., 2004
Formaldehyde	Formaldehyde dehydrogenase	Carbon cloth	-	+0.1 V vs. SCE	2	20-250	-	Campbell and Roshpon, 2000
Sorbitol	Sorbitol dehydrogenase				2	6.5-200	-	
Ethanol	Alcohol dehydrogenase	Fe_2O_3 /CB	-	+0.00 V vs. Ag/AgCl	-	0-1500	0.06 μA mM^{-1}	Kim et al., 2009
Ethanol	Alcohol dehydrogenase	GC	Titanium containing MCM-41 (Ti-MCM 41)	+0.28 V vs. SCE	10	25-1000	-	Dai et al., 2007
Glucose	Glucose dehydrogenase	GC	Highly ordered mesoporous carbon (MOCs)	+0.35 V vs. Ag/AgCl	-	500-15000	0.053 nA $μM^{-1}$	Zhou et al., 2008
Ethanol	Alcohol dehydrogenase	Au	Self-assembled monolayers (SAMs) of thiocytosine (Au-TC)	+0.00 V-+0.70 V vs. Ag/AgCl	-	-	3.435±0.04 μA cm^{-2} mM^{-1}	Raj and Behera, 2005
			Self-assembled monolayers (SAMs) of mercaptopyrimidine (Au-MPM)		-	-	3.24±0.03 μA cm^{-2} mM^{-1}	
			Self-assembled monolayers (SAMs) of 4-amino-2-mercaptopyrimidine (Au-AMP)	+0.00 V-+0.8 V vs. Ag/AgCl	-	-	1.307±0.04 μA cm^{-2} mM^{-1}	Behera and Raj, 2007

NADH biosensor

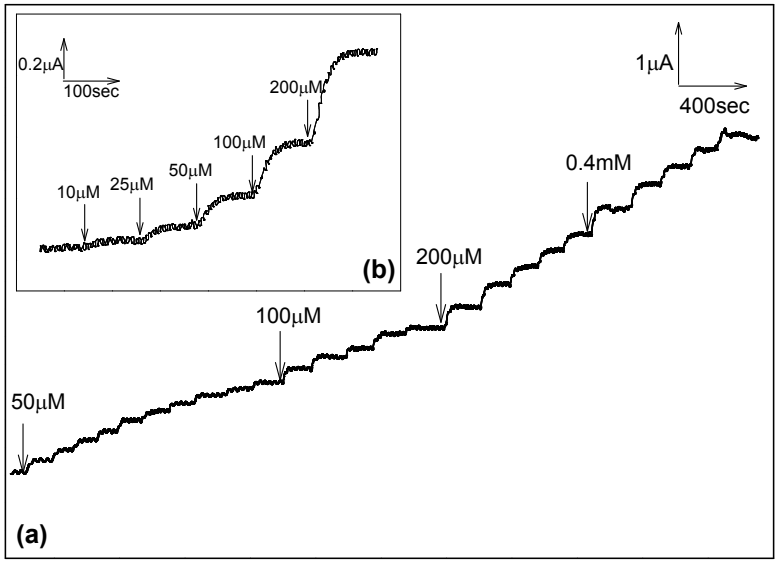

Figure. (a), (b) Amperometric response of the carbon black-iron oxide electrode with different NADH concentration at 0.00V.

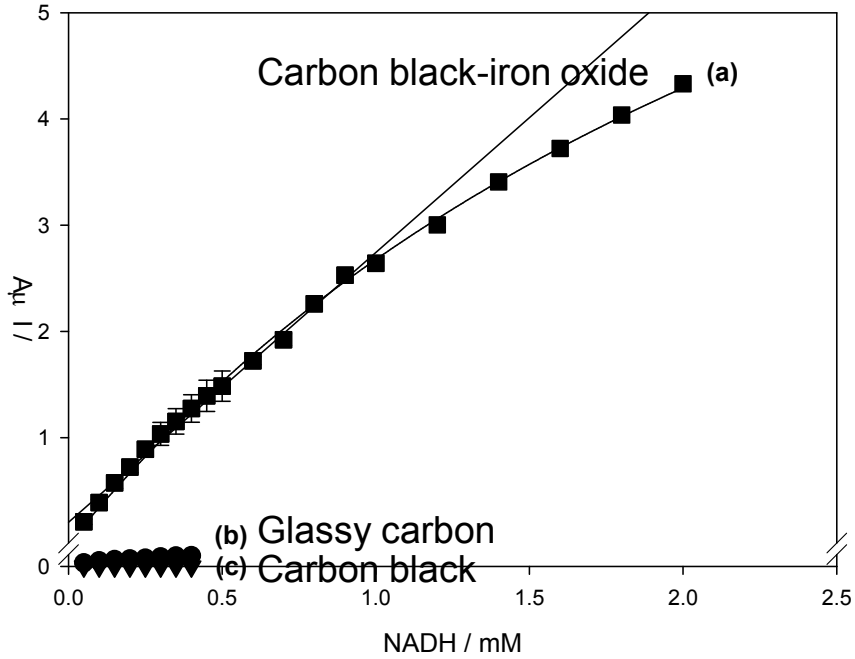

Figure. Calibration curve for NADH oxidation at (a)carbon black-iron oxide electrode, (b) glassy carbon, and (c) carbon black at 0.00V.

- ✓ Linear range 10μM-1000μM (R^2=0.993)
- ✓ Limit of detection (LOD) 10μM (S/N=3)
- ✓ Sensitivity 2.54 μA mM^{-1}
- ✓ Km=3.04mM

Ethanol biosensor

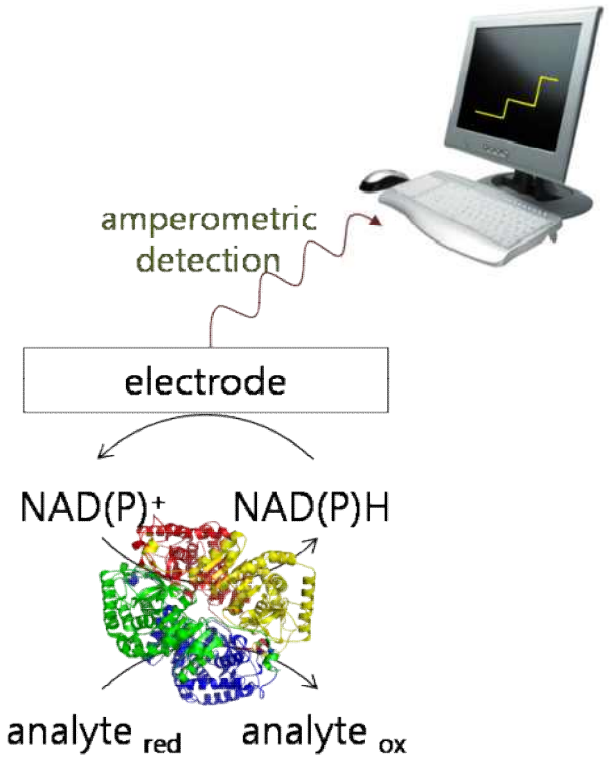

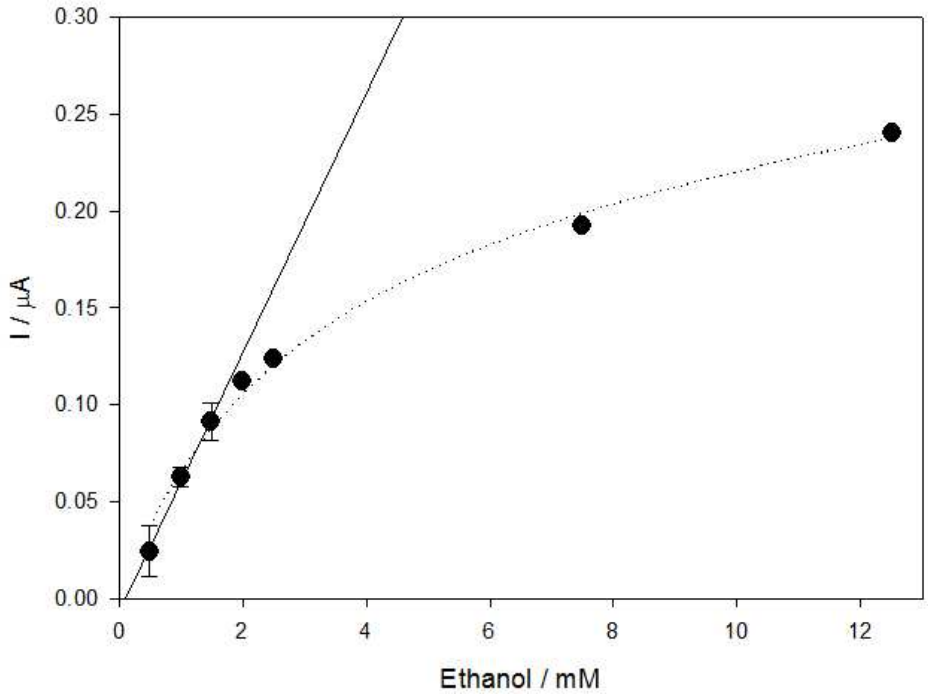

Figure. Calibration curve for ethanol at carbon black-iron oxide electrode at 0.00V (C_{ADH}=2mg/5ml, C_{NAD}+=10mM).

Enzyme fuel cell

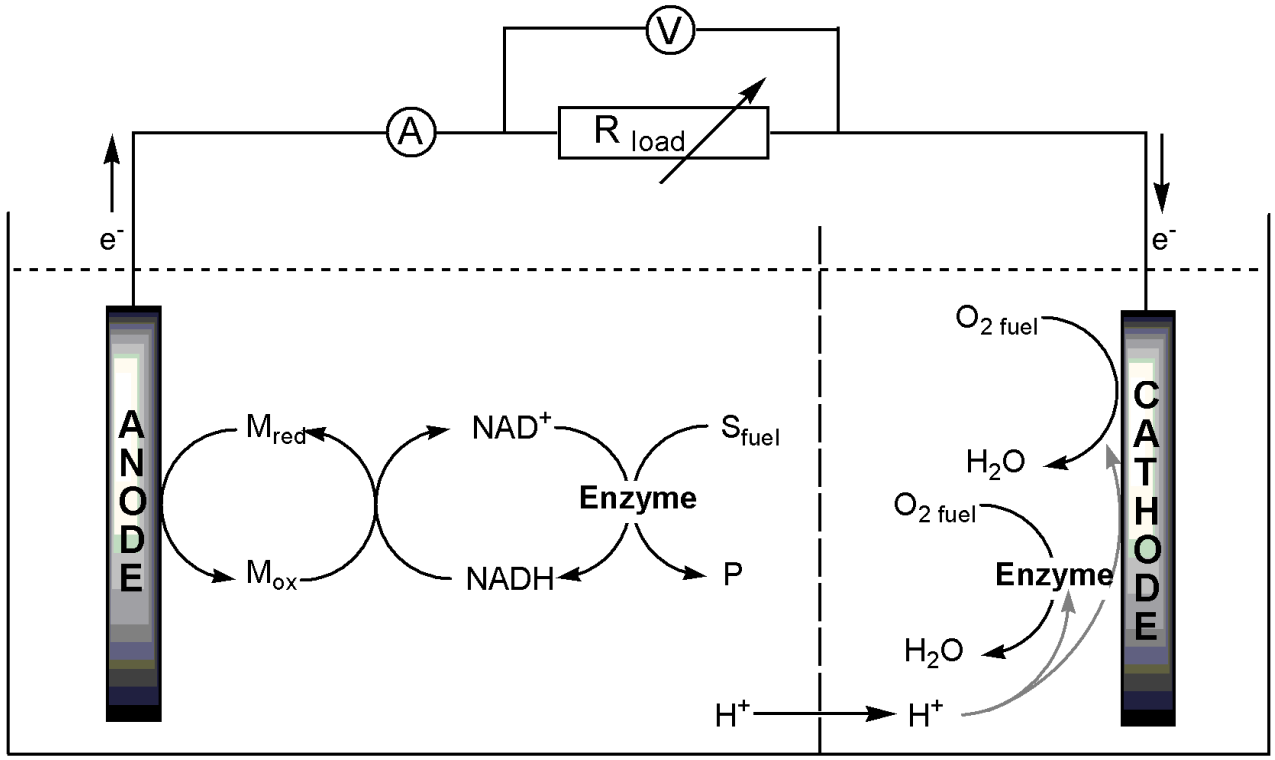

Fuel	Anode	Cathode	Open circuit voltage [V]	Current density [$\mu A\ cm^{-2}$]	Power density [$\mu W\ cm^{-2}$]	Reference
Glucose (80 mM)/O_2	D-glucose dehydrogenase (NAD^+) Meldola Blue (MB^+) modified graphite disc (A=16 cm^2) 0.25 M phosphate buffer (pH 7.0)	Pt gauze 0.37 M phosphate buffer (pH 7.0)	+0.8	200	-	Persson et al., 1985
Methanol (100 mM)/O_2	Alcohol dehydrogenase/ aldehyde dehydrogenase/formate dehydrogenase (NAD^+) Benzyl Viologen (BV^{2+})/diaphorase Graphite plate (A=2 cm^2) 1 M LiCl in 0.1 M tris buffer (pH 7.5)	Pt gauze (3 cm^2) 1 M LiCl in 0.1 M tris buffer (pH 7.5)	+0.8	-	680 (at 490 mV)	Palmore et al., 1998
Lactate (20 mM)/O_2	Lactate dehydrogenase (NAD^+) Integrated LDH/NAD^+/PQQ immobilized on gold (A=0.2 cm^2) 0.01 M $CaCl_2$ in 0.1 M Tris buffer (pH 7.0)	Cytochrome c/cytochrome oxidase linked to the gold (A=0.2 cm^2)	-	-	4.1 (w/o magnetic field) 12.4 (w/ magnetic field)	Katz et al., 2005
Glucose (40 mM) /O_2 Ethanol (60 mM)/O_2	Glucose dehydrogenase ($NADP^+$) Alcohol dehydrogenase (NAD^+) GDH/$NADP^+$/Nile Blue/SWCNTs on glassy carbon (φ=3 mm) 0.1 M phosphate buffer (pH 7.0)	Bilirubin oxidase BOD/SWCNTs on glassy carbon (φ=3 mm) 0.1 M phosphate buffer (pH 7.0)	-	-	23 (glucose/O_2) 48 (EtOH/O_2)	Yan et al., 2007
Ethanol (1 mM) /O_2 Methanol (1 mM)/O_2	Alcohol dehydrogenase (NAD^+) Aldehyde dehydrogenase (NAD^+) Formaldehyde dehydrogenase (NAD^+) Formate dehydrogenase (NAD^+) Poly(methylene green) modified carbon felt (A=1 cm^2) Phosphate buffer (pH 7.15)	ELAT (gas diffusion electrode, 1 mg cm^{-2} Pt loading) Phosphate buffer (pH 7.15)	0.60-0.62 (ADH; EtOH) 0.82 (ADH/AlDH; EtOH) 0.71 (ADH/FalDH/FDH; MeOH)	-	1160 (ADH; EtOH) 2040 (ADH/AlDH; EtOH) 1550 (ADH/FalDH/FDH; MeOH)	Akers et al., 2005
Ethanol (1 mM) /O_2	Alcohol dehydrogenase (NAD^+) Aldehyde dehydrogenase (NAD^+) Poly(methylene green) modified glassy carbon (φ=3 mm)	Bilirubin oxidase BOD/$Ru(bpy)_3^{2+}$ Carbon fiber paper (A=1 cm^2)	0.68±0.1 (Nafion®) 0.51±0.11 (membraneless)	-	830±160 (Nafion®) 390±60 (membraneless)	Topcagic and Minteer, 2006
Lactate (20 mM)/H_2O_2	Lactate dehydrogenase (NAD^+) LDH/PQQ immobilized on gold (φ=2 mm) 20 mM $CaCl_2$ in 0.1 M Tris buffer (pH 7.0)	Microperoxidase ABTs/MP-11 immobilized on gold (φ=2 mm) 20 mM $CaCl_2$ in 0.1 M Tris buffer (pH 7.0)	-	-	142	Lee et al., 2008